



Original Research Article

Mapping of Lineaments Structures for Groundwater Study using Aeromagnetic Data: Case Study of a part of Ilorin and its Adjoining Areas, Central Nigeria

Olawuyi, A. K.1* and Oddiah, O. A.2

1 Department of Applied Geophysics, University of Ilorin, Ilorin, Nigeria

2 Department of Geology and Mineral Sciences, University of Ilorin, Nigeria

*Corresponding Author: olawuyi.ak@unilorin.edu.ng

Article History:

Received: September 16, 2023

Accepted: January 12, 2024

Published: January 20, 2024

Copyright: © 2024 by the authors.

This is an open-access article distributed under the terms of the Creative Commons Attribution License

(<https://creativecommons.org/licenses/by/4.0/>)

Print ISSN 2710-0200

Electronic ISSN 2710-0219

ABSTRACT

A study was conducted on the Basement Complex rocks around Ilorin, located in southwestern Nigeria, to map lineaments and understand the structural elements influencing the region's hydrogeology. The investigation combined aeromagnetic data analysis with existing geological information from the area. Both qualitative and quantitative approaches were applied using *Oasis Montaj™* software to interpret the IGRF-corrected aeromagnetic dataset. Depth estimation to magnetic sources was carried out through three-dimensional (3D) Euler deconvolution, which provided insights into source geometry, magnetic characteristics, and subsurface structural configurations based on structural indices. The integration of aeromagnetic interpretations with geological data enabled the extraction and evaluation of major lineaments and fault systems. The analysis revealed that many of the delineated structural features align with river channels depicted on geological maps, suggesting a strong structural influence on the drainage pattern. Predominant lineament orientations are NE-SW, with subordinate NW-SE trends, reflecting conjugate strike-slip fault systems associated with the Pan-African tectonic events in Nigeria. These structures display both dextral and sinistral movements, cross-cutting earlier Pan-African fabrics.

Keywords: 3D Euler Deconvolution, Lineaments, Qualitative, Quantitative, anomalies.

INTRODUCTION

Airborne magnetic surveys have become one of the most valuable tools in regional investigations of Precambrian basement terrains. This geophysical approach is particularly effective in distinguishing lithological units and structural patterns that arise from lateral variations in the magnetic properties of crystalline rocks (Okpoli, 2019).

Over time, numerous analytical methods have been developed for fault and lineament characterization. These include two-dimensional forward modeling and inversion (Talwani et al.,

1959) as well as Euler deconvolution (Reid et al., 1990; FitzGerald et al., 2004). Subsequent refinements and modifications to Euler deconvolution techniques for potential field data interpretation were introduced by Keating (1998), Mushayandebvu et al. (2004), and other researchers.

The application of potential field methods—particularly gravity and magnetic techniques—has a long history in geoscientific exploration. These methods have been used extensively to delineate subsurface structures for mineral and energy resource exploration, including coal, hydrocarbons, and metallic ores such as gold and diamonds. Beyond resource prospecting, they are also applied in hydrogeological, environmental, and geotechnical investigations, often serving as reconnaissance tools that guide more detailed surveys (Kearey et al., 2004). Automated interpretation procedures, such as spectral analysis and Euler deconvolution, have proven effective for processing large datasets to delineate local anomalies. These techniques assume that observed anomalies originate from relatively simple geometric sources—such as monopoles, dipoles, or dipole lines—and can estimate the depth and position of causative bodies, which in turn facilitates more detailed subsurface modeling.

Recent technological advancements have further enhanced the precision of magnetic anomaly interpretation across broad regions. Developments in data acquisition systems, GPS-based navigation, and advanced statistical approaches (Dods et al., 1985) have substantially improved the resolution of total magnetic field measurements and their gradients. As a result, higher-order derivative techniques—such as second and third derivatives—can now be applied effectively to reveal subtle subsurface features (Nabighian et al., 2005).

Various interpretation approaches have been designed to determine source depth, magnetization, and geometry of magnetic bodies. Semi-automatic profile analysis techniques were earlier proposed by Nabighian (1972, 1974), Atchuta Rao et al. (1981), and Thompson (1982), while subsequent studies extended these concepts into three-dimensional modeling suitable for gridded datasets (Nabighian, 1984; Blakely & Simpson, 1986; Reid et al., 1990; Wang & Hansen, 1990). Among these, Euler deconvolution has emerged as a widely utilized method, evolving significantly from its original two-dimensional application by Thompson (1982) to its three-dimensional formulation by Reid et al. (1990). The technique provides automated estimates of source positions and depths, and has been extensively applied to magnetic datasets by numerous researchers and institutions (e.g., Ravat, 1996; Reid et al., 1990), though its use in gravity interpretation remains comparatively limited.

Several studies have investigated the structural and tectonic evolution of the Nigerian Basement Complex using aeromagnetic data (Ajakaiye et al., 1986; Balogun, 2019; Osagie et al., 2021). Building upon this foundation, the present study applies 3D Euler deconvolution to aeromagnetic data acquired over Ilorin and its adjoining regions in southwestern Nigeria. The study explores the hydrogeological implications of the identified faults and lineaments, emphasizing their relationship with structurally controlled drainage systems and aquifer distributions. The methodological simplicity demonstrated here may encourage the adoption of this approach in other regions with comparable geological settings.

MATERIALS AND METHODS

Location and Geologic Setting

The investigated area forms part of Ilorin, corresponding to Sheet 223 of the Nigerian topographical map. Each map sheet represents a $\frac{1}{2}^\circ$ by $\frac{1}{2}^\circ$ quadrangle at a scale of 1:100,000.

Geographically, the study area extends between latitudes 08°27'N and 08°30'N, and longitudes 04°31'E and 04°38'E, covering an approximate surface area of 70.45 km² within Ilorin, the capital city of Kwara State, Nigeria (Figure 1).

According to Balogun (2019), the lithology of the area is dominated by rocks of the Migmatite–Gneiss–Quartzite Complex, which constitute roughly 75% of the exposed formations. These include migmatitic gneiss, banded gneiss, granite gneiss, and quartzite units. The remaining 20% of the rock assemblage belongs to the Younger Metasedimentary Series, represented mainly by schist and flaggy quartzite (Figure 1). The Younger Metasediments are restricted primarily to the southeastern portion of the map area, whereas the Migmatite–Gneiss–Quartzite Complex extends eastward beyond the mapped region to localities such as Ajegunle, Oke-Baba, Ilofa, and Eruku, which fall outside the present study limits.

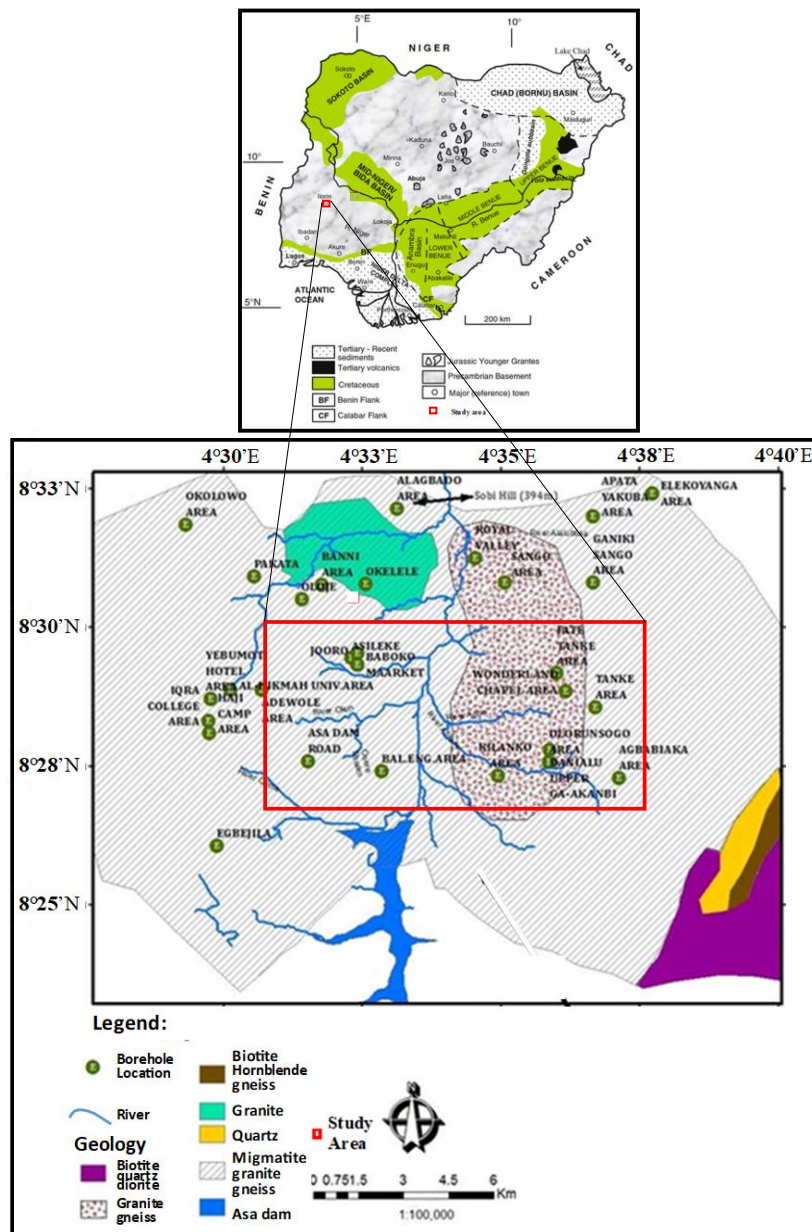


Figure 1: The geologic map of Ilorin and its adjoining areas (After Ashaolu, 2016, Inset is the geological sketch map of Nigeria, After Obaje, 2009)

Aeromagnetic Data

The dataset utilized for this investigation consists of high-resolution aeromagnetic data gridded at $100\text{ m} \times 100\text{ m}$ intervals (Total Magnetic Intensity, TMI) as illustrated in Figure 2. The survey, conducted by the Nigerian Geological Survey Agency (NGSA) in 2006, was flown at an average terrain clearance of 80 m. The aeromagnetic data corresponding to Ilorin (Sheet 223) were obtained from the NGSA headquarters in Abuja. The primary objective of the original survey was to enhance geological mapping for mineral and groundwater resource development.

Survey parameters included a flight altitude of 80 m, a line spacing of 500 m for flight lines, and 2000 m for tie lines. The flight lines were oriented in a NW-SE direction, while the tie lines trended NE-SW. For data standardization, a constant base value of 32,000 nT was subtracted from all measurements. This offset can be added back to each data point to recover the absolute regional magnetic field, although it does not influence the internal relationships or geometry of the grid since the subtraction is uniform across the dataset. To account for the geomagnetic field conditions prevailing at the time of acquisition, the 2005 epoch of the International Geomagnetic Reference Field (IGRF) was adopted. The calculated parameters for the study area were: total field strength = 33,129.9632 nT, inclination = -6.8734° , and declination = -2.5136° . The TMI data were subsequently reduced to the magnetic equator (REDE) in order to minimize asymmetry effects caused by low-latitude magnetic anomalies (Figure 3).

Both the TMI and REDE maps emphasize short- and long-wavelength magnetic variations that reflect lithological boundaries, structural orientations, and magnetization contrasts within the subsurface. Distinct magnetic anomalies observed in these maps correspond to discrete magnetic zones and provide the basis for further interpretation of the subsurface structural framework of the area.

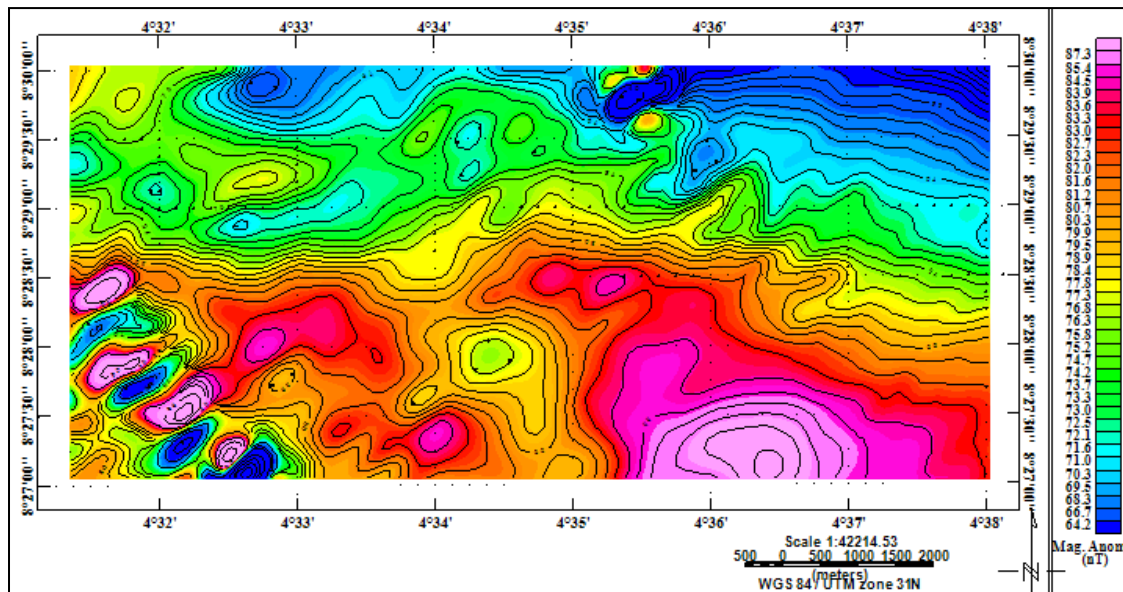


Figure 2: TMI map of the Study area

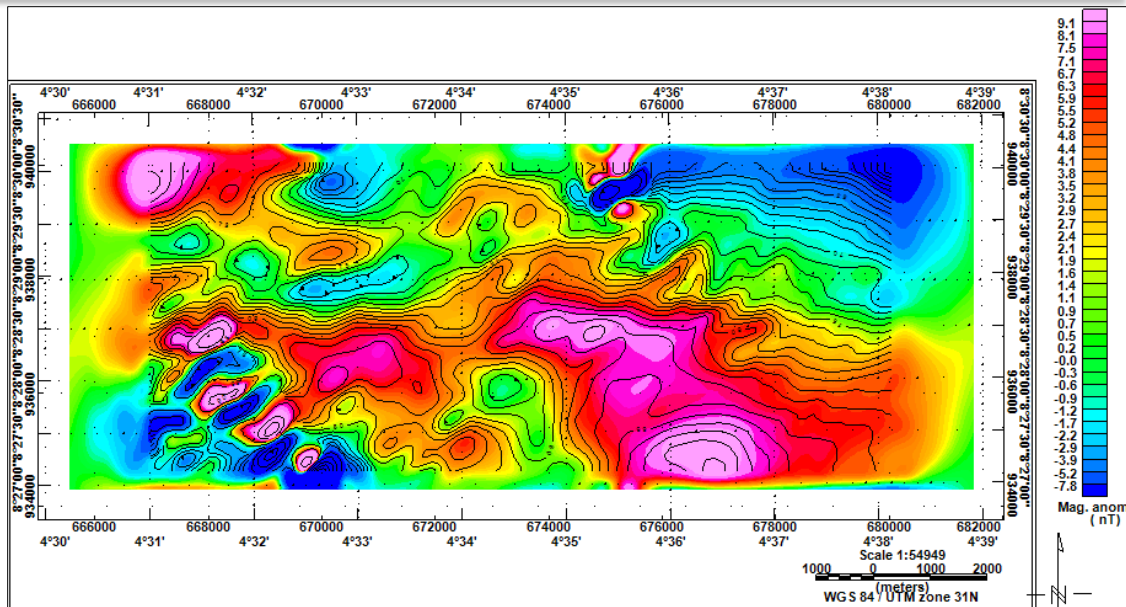


Figure 3: The Reduced to Equator (REDE) map of the Study area

Euler Deconvolution

The 3D Euler deconvolution technique was used on the aeromagnetic data to provide estimates of depths to anomalies sources and determine the source location (x_0, y_0, z_0) through the inversion of the Euler's homogeneity equation over a window of data.

The 3D Euler deconvolution technique is an equivalent method based on the Euler's homogeneity equation as developed by Reid *et al.* (1990) following Thompson's (1973) suggestion and operating on gridded magnetic data. The method is based on the concept that anomalous magnetic fields of localized structures are homogeneous function of the source coordinate and, therefore, satisfies Euler's homogeneity equation. The method operates on the data directly and provides a mathematical solution without recourse to any geological constraints. The application of Euler deconvolution has emerged as a powerful tool for direct determination of depth and probable source geometry in magnetic data interpretation (Barbosa *et al.*, 1999). The Euler derived interpretation requires only a little *a priori* knowledge about the magnetic source geometry and information about the magnetization vector (Barbosa *et al.*, 2000).

The 3-D Euler Deconvolution processing routine is an automatic location and depth determination software package for gridded magnetic and gravity data (Oasis montaj™). The depths are displayed as a grid and are based on source parameters of the following source models: contacts (faults), thin sheets (dykes) or horizontal cylinders. The relationship between structural index (η), type of magnetic/gravity model and position of the calculated depth as described by Hsu (2002) is presented in the Table 1. The structural index for gravity model is one less than that of magnetic and the maximum for gravity is 2.

Table 1: The Relationship Between Structural Index (n), Type of Magnetic/Gravity Model and Position of the Calculated Depth (After Hsu, 2002).

Structural index (n)	Type of magnetic model	Type of gravity model	Position of Euler depth (m)
0.0	Contact with large depth extent	Sill/Dyke/Step	At top and edge
0.5	Contact with small depth extent	Ribbon	
1.1	Thin prism with large depth	Pipe	At top and centre or at edge and half throw
2.0	Vertical or horizontal cylinder	Sphere	At centre
3.0	Sphere		

Theory of Euler Deconvolution Method:

According to Whitehead and Musselman, (2005) ‘Any three-dimensional function $f(x,y,z)$ is said to be *homogeneous* of degree n if the function obeys the expression:

$$f(tx,ty,tz)=t^n f(x,y,z) \quad (1)$$

From this it can be shown that the following (known as *Euler’s equation*) is also satisfied:

$$x \frac{\partial f}{\partial x} + y \frac{\partial f}{\partial y} + z \frac{\partial f}{\partial z} = nf \quad (2)$$

Thompson (1982) has shown that simple magnetic and gravity models conform to Euler’s equation. The degree of homogeneity, n , can be interpreted as a *structural index* (SI). Reid *et al.* (1990) have shown that a magnetic contact will yield an index of 0.5 provided that an offset A is introduced to incorporate an anomaly amplitude, strike and dip factors (Whitehead and Musselman, 2005):

$$A = (x - x_0) \frac{\partial T}{\partial x} + (y - y_0) \frac{\partial T}{\partial y} + (z - z_0) \frac{\partial T}{\partial z} \quad (3)$$

Given a set of observed total field data, we can determine an optimum source location (x_0, y_0, z_0) by solving Euler’s equations for a given index n by least-squares inversion of the data.

RESULTS AND DISCUSSION

Depth Estimation: 3-D standard Euler deconvolution

Zone Coloured Euler Solutions for Different Geologic Structures- The structural indices 0.0 to 3.0 (i.e. faults with large depth to sphere model; magnetic), represent the different geologic structures. In the Ilorin study area, Figures 4a and b show the results obtained for structural indices of 0.0 (i.e. faults/steps, dykes and sills model (near surface); magnetic) and 0.5 (i.e. faults/steps, dykes and sills model (deep seated); magnetic). In Oasis montaj™, window size determination is either by default (i.e. 20 x 20) or through iterations, as the correct SI for a given feature will give the tightest clustering of solutions or sharpest focus of results. The structural index 0.0 and 0.5 (magnetic) of 3D Euler Deconvolution has been used worldwide to detect the near surface and deep seated faults/steps, dykes and sills model (Kearey *et al.*, 2004 and Olawuyi *et al.*, 2016). Also, Figures 5a and b show the superimposition of faults and lineaments obtained from 3D Euler solutions on the drainage map of the study area. Many of these channels coincided with the Euler solutions clusters, confirming that the drainage in the study area is structurally

controlled. The fact that both features are oriented mostly in the NE-SW followed by NW-SE directions corroborate the fact that the Pan African in Nigeria was followed by conjugate strike slip fault systems which averaged in the NE-SW and NW-SE directions and showed dextral and sinistral sense of displacement which cut across the earlier Pan African structures (Ball, 1980).

The abundance of lineament structures in Ilorin and its adjoining areas is an indication that the area is potentially viable for groundwater exploration. 'The groundwater flow in fractured bedrock aquifers is predominantly through fractures, with large-scale fracture zones and faults acting as conduits for flow at the regional scale' (Denny *et al.*, 2007).

CONCLUSION

Airborne magnetic datasets over Ilorin and its environs, in Central Nigeria were collected and processed. The IGRF corrected TMI map was reduced to the equator and processed with 3D Euler deconvolution subroutine of Oasis montaj™. Using the appropriate structural indices, the lineament structures within the Ilorin and its adjoining areas were identified and correlated with the drainage map. The lineaments structures did not only coincide with the river channels but were both aligned mostly in the NE-SW followed by the NW-SE directions, showing that the drainage is not only structurally controlled but corroborates the fact that 'the Pan African in Nigeria was followed by conjugate strike slip fault systems which averaged in the NE-SW and NW-SE directions and showed dextral and sinistral sense of displacement which cut across the earlier Pan African structures' (Ball, 1980).

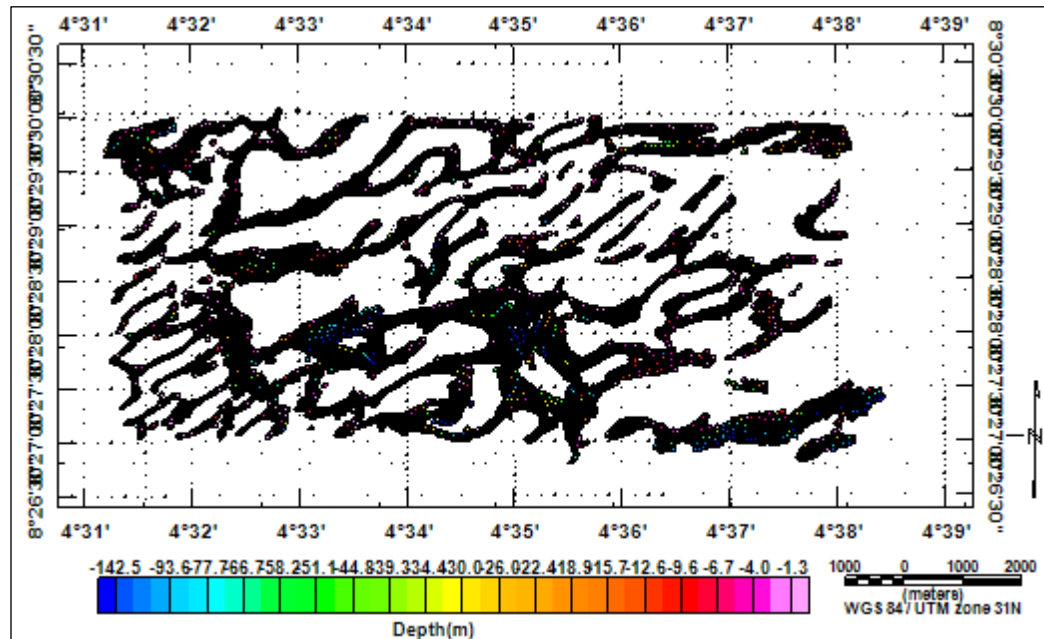


Figure 4a: Result of Euler Deconvolution of Aeromagnetic Data of Ilorin and its adjoining areas (SI=0.0).

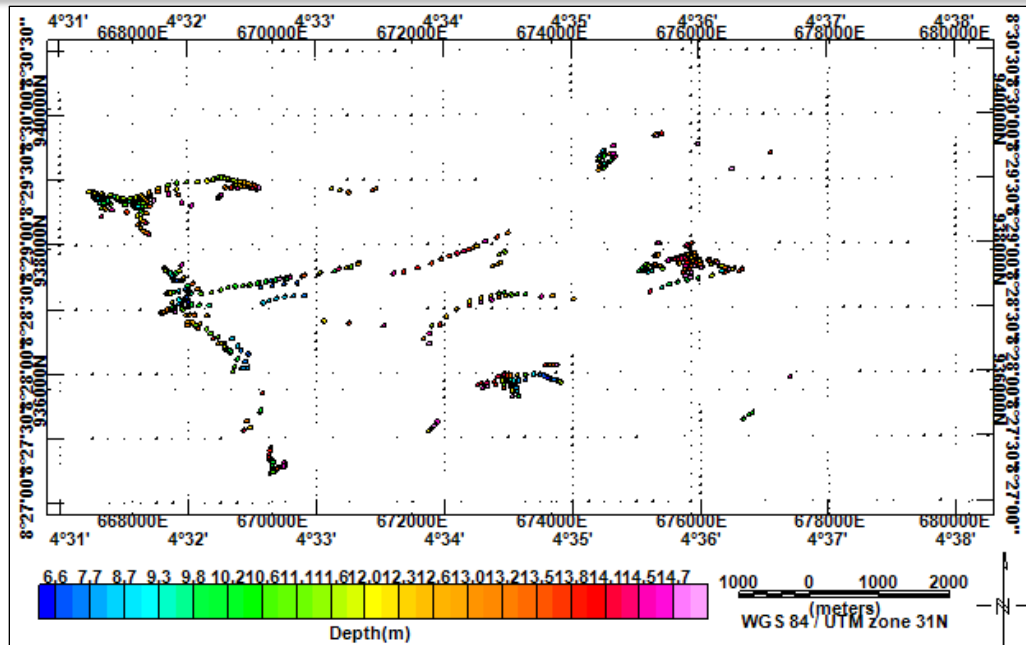


Figure 4b: Result of Euler Deconvolution of Aeromagnetic Data of Ilorin and its adjoining areas (SI: 0.5)

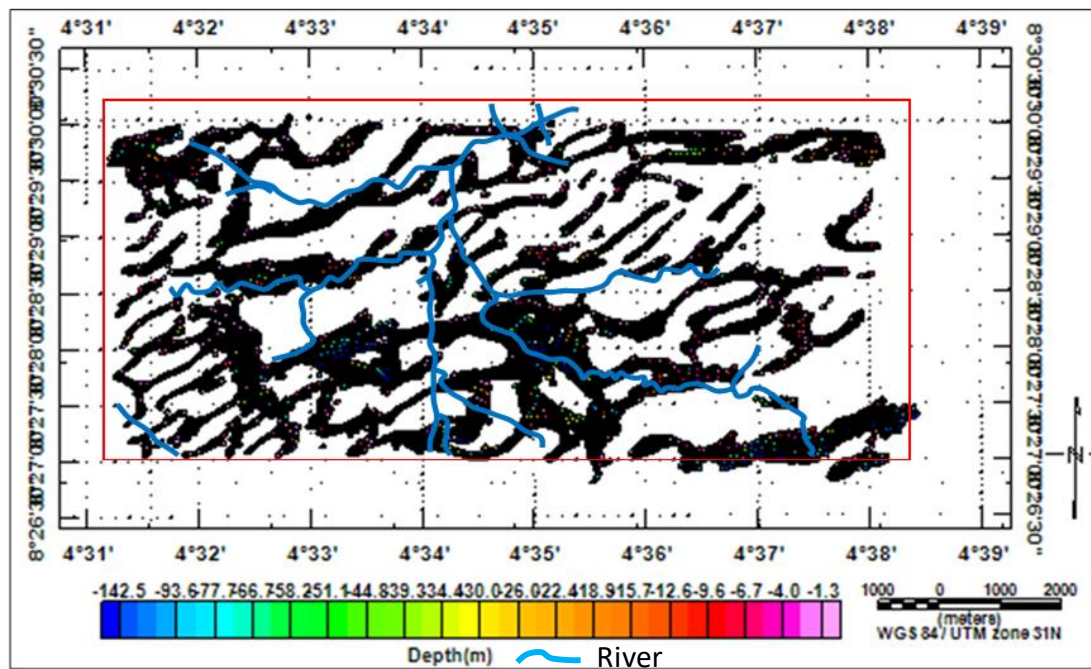


Figure 5a: Superimposition of Result of Euler Deconvolution of Aeromagnetic Data of Ilorin and its adjoining areas (SI=0.0) over the drainage map.

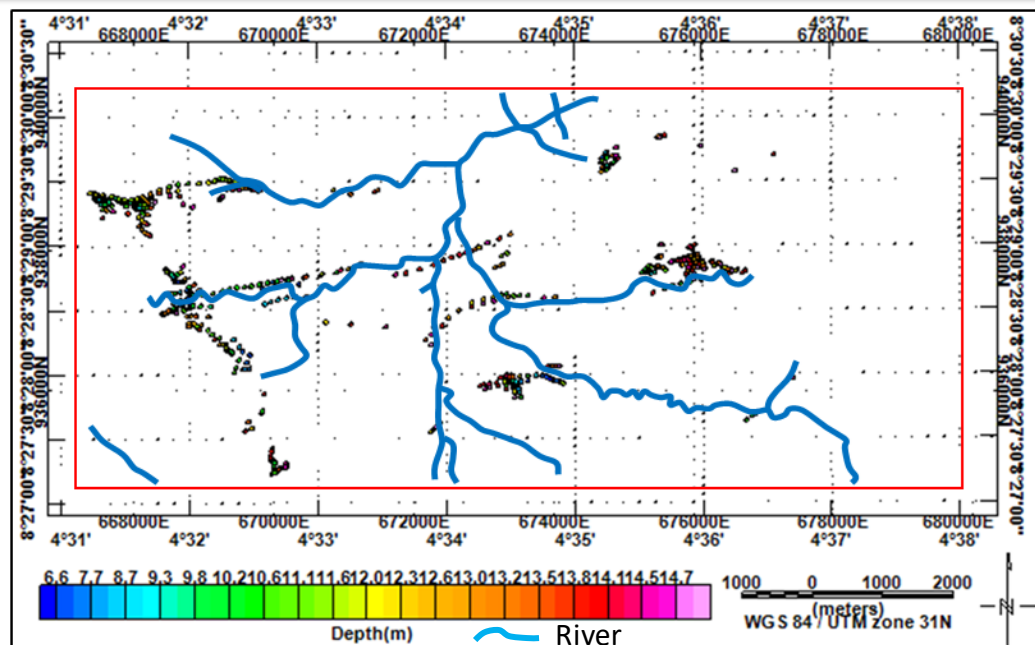


Figure 5b: Superimposition of Result of Euler Deconvolution of Aeromagnetic Data of Ilorin and its adjoining areas (SI: 0.5) over the drainage map.

The abundance of lineament structures in Ilorin and its adjoining areas could also imply that the area under study is potentially viable for groundwater exploration.

REFERENCES

- Ajakaiye, D. E., Hall, D. H. and Millar, T. W. (1989). Interpretation of Aeromagnetic Data Across the Central Crystalline Shield Area of Nigeria; *Geology of Nigeria*; edited by Kogbe; View Limited (Publisher) Jos, Nigeria. pp. 347-358.
- Ashaolu, D. E., Ifabiyi, I. P. and Omotosho, O. (2016). Hydrogeological Characteristics of Groundwater Yield in Shallow Wells of the Regolith Aquifer: A Study from Ilorin, Nigeria. *Mamona Etyhiopian Journal of Science*, **8**(1): 23-36. DOI:10.4314/mejs.v8i1.2
- Atchuta Rao, D., Ram Babu, H. V., and Sanker Narayan P. V. (1981). Interpretation of magnetic anomalies due to dikes: The complex gradient method: *Geophysics*. **4**(6): 1572- 1578.
- Ball, E. (1980). An example of very consistent brittle deformation over a wide intra-continental area: The late Pan African fracture system of the Tuareg and Nigerian shield. *Tectonophysics* **61**: 363-379.
- Barbosa, V.C.F., Silva, J.B.C., Medeiro, W.E. (1999). Stability analysis and improvement of structural index estimation in Euler deconvolution. *Geophysics*, **64**: 48-60.
- Barbosa, V.C.F., Silva, J.B.C. and Medeiros, W.E. (2000). Making Euler deconvolution applicable to small ground magnetic surveys. *J. Applied Geophysics*. **43** (1): 55-68.
- Balogun, O. B. (2019). Tectonic and structural analysis of the Migmatite–Gneiss–Quartzite complex of Ilorin area from aeromagnetic data, *NRIAG Journal of Astronomy and Geophysics*, **8**(1):1,22-33, DOI: 1080/2090977.2019.1615795
- Blakely, R. J. and Simpson, R. W. (1986). Approximating edges of Source bodies from magnetic or gravity anomalies: *Geophysics*, **51**: 1494–1498.

- Denny, S.C., Allen, D.M. and Journeay, A.M. (2007). DRASTIC-Fm: A Modified Vulnerability Mapping Method for Structurally Controlled Aquifers in the Southern Gulf Islands, British Columbia, Canada. *Hydrogeology Journal*, 15: 483-493. DOI 10.1007/s10040-006-0102-8.
- Dods, S. D., Teskey, D. J., and Hood, P. J. (1985). The new series of 1: 1,000,000-scale magnetic anomaly maps of the Geological Survey of Canada: Compilation techniques and Interpretation.
- FitzGerald, D., A. Reid, and McInerney, P. (2004). New discrimination techniques for Euler deconvolution: Computer and *Geoscience*, **30**: 461–469.
- Hsu, S.K. (2002). Imaging Magnetic Sources Using Euler's Equation. *Geophysical Prospecting*, **50**: 15 – 25.
- Keating, P. B. (1998). Weighted Euler deconvolution of gravity data. *Geophysics*, 63,1595-1603.
- Kearey, P., Brooks, M. and Hill, I. 2004. An Introduction to Geophysical Exploration (3rd edn). Blackwell Science, Oxford. 262pp.
- Mushayandebvu, M. F., Lesur, V., Reid, A. B. and Fairhead, J. D. (2004). Grid Euler Deconvolution with Constraints for 2D Structures: *Geophysics*, **69**: 489–496. doi:10.1190/1.1707069.
- Nabighian, M. N. (1972). The analytic signal of two-dimensional Magnetic bodies with polygonal cross-section — Its properties and use for automated anomaly interpretation: *Geophysics*, **37**: 507–517.
- Nabighian, M.N. (1974). Additional comments on the analytic signal of two dimensional magnetic bodies with polygonal cross-section: *Geophysics*, **39**: 85–92.
- Nabighian, M.N. (1984). Toward a three-dimensional automatic interpretation potential field data via generalized Hilbert transforms—Fundamental relations: *Geophysics*, **49**: 780–786.
- Nabighian, M.N., Grauch, V.J.S., Hansen, R.O., LaFehr, T.R., Li, Y., Peirce, J.W., Phillips, J.D., Ruder, M.E. (2005). The historical development of the magnetic method in exploration. *Geophysics*, **70**: 33-61.
- Obaje, N. G. (2009). Geology and Mineral Resources of Nigeria, Lecture Notes in Earth Sciences 120. Springer-Verlag, Berlin. <http://dx.doi.org/10.1007/978-3-540-92685-6>
- Okpoli, C. C. (2019). High Resolution Magnetic Field Signatures Over Akure and its Environs, Southwestern Nigeria. *Earth Sciences Malaysia (ESMY)* DOI: <http://doi.org/10.26480/01.2019.09.17>
- Olawuyi A.K., Ako B.D., Omosuyi G.O. and Adelusi A.O. (2016). Application of 3-D Euler Deconvolution of Aeromagnetic and Pseudogravity Transforms in Mineral Exploration: A Case Study of the Pegmatite-Rich Zones of Lafiagi, Central Nigeria. *Arabian J. Geosci.* **9**(16): 1-9.
- Osagie, A. U., Eshanibli, A. and Adepelumi, A. A. (2021). Structural trends and basement depths across Nigeria from analysis of aeromagnetic data. *Journal of African Earth Sciences*. 178 (104184).
- Ravat, D. (1996). Analysis of the Euler method and its applicability in environmental magnetic investigations: *Journal of Environmental and Engineering Geophysics*, **1**: 229–238. doi:10.4133/JEG1.3.229
- Reid, A.B., Allsop, I.M., Grsner, H., Millet, A.J., Somerton, I.W. (1990). Magnetic interpretation in three dimensions using euler deconvolution. *Geophysics*, **55**: 80-91.
- Talwani, M. Worzel, J.L. and Landisman, M. (1959). Rapid gravity computations for two-dimensional bodies with applications to the Mendocino submarine fracture zones. *J. Geophys. R.*, **64**: 49 - 59.

- Thompson, D.T. (1973). Identification of Magnetic Source Types Using Equivalent Simple Models: Presented at the 1973 Fall Annual AGU Meeting in San Francisco.
- Thompson, D.T. (1982). EULDPH-A New Technique for Making Computer Assisted Depth Estimates from Magnetic Data. *Geophysics*, **47**: 31-37.
- Wang, X., and Hansen, R. O. (1990). Inversion for magnetic anomalies of arbitrary three-dimensional bodies: *Geophysics*, **55**: 1321-1326.
- Whitehead, N. and Musselman C. (2005). Montaj Grav/Mag Interpretation. Processing, Analysis and Visualization system for 3D Inversion of Potential Field Data for Oasis Montaj™, Tutorial and User Guide, Version 6.1, Geosoft Inc. Toronto, ON Canada M5J 1A7.